Influence of the reducing agents on morphology and properties of silver structures on paper

Nguyen Thi Bich Ngoc[1, 2, *]**, Nguyen Thi Thuy**[1]**, Nguyen Trong Nghia**[1]**,**
Nguyen Duc Toan[1, 2]**, Dao Duc Manh**[3]**, Chu Viet Ha**[4, *]**, Nghiem Thi Ha Lien**[1]

[1]*Institute of Physics, Vietnam Academy of Science and Technology, 18 Hoang Quoc Viet, Cau Giay, Ha Noi, Viet Nam*

[2]*Graduate University of Science and Technology, Vietnam Academy of Science and Technology, 18 Hoang Quoc Viet, Cau Giay, Ha Noi, Viet Nam*

[3]*Hanoi Pedagogical University 2, Xuan Hoa, Phuc Yen city, Vinh Phuc, Viet Nam*

[4]*Thai Nguyen University of Education, 20 Luong Ngoc Quyen, Thai Nguyen city, Thai Nguyen, Viet Nam*

[*]Emails*: ntbngoc@iop.vast.vn, chuvietha@tnue.edu.vn*

Abstract. Paper-based SERS substrates (PSSs) with tunable plasmonic properties and excellent flexibility have been applied in various fields. These SERS substrates were prepared using a direct chemical reduction synthesis method for the present work. By using various types of reducing agents (RAs): (1) sodium borohydride ($NaBH_4$), (2) ascorbic acid (L-AA), (3) glucose, and (4) formaldehyde (HCHO), the silver nanostructures (AgNS) on cellulose paper fiber was fabricated with the morphologies. Morphological research results have shown that with strong RAs, AgNS on paper substrates have a spherical shape. In contrast, with weak RAs, ANS on paper substrates have an anisotropic morphology which depends on the crystal surface development priority. Specifically, AgNS generated on paper using glucose have a bar shape and thin planar silvery-wing shape when using the reducing agent L-AA. The plasmon characterization of AgNS on paper was systematically investigated by the diffuse reflectance spectroscopy. The fabricated paper-based SERS substrates were used to detect melamine in an aqueous solution and to determine the influence of type RAs on the enhancement factor (EF) and signal uniformity of SERS substrates. Among the four types of RAs, the SERS substrates used $NaBH_4$ have the highest SERS signal with the limit of detection of 10^{-8} M for melamine and the EF = 2.3×10^9.

1. INTRODUCTION

In recent years, nanotechnology research has been proliferating and used in various fields. One of the attractive aspects of the nanoscale is the dependence of properties on the size and shape of the material. Especially, plasmonic metals display a rich plasmon behavior that can be tuned via variation in size and shape [1]. These plasmonic metals can produce enhanced electromagnetic fields through the excitation of localized surface plasmon resonances (LSPR). By this characteristic, the materials have been widely used in chemical and biological sensing fields, such as detection techniques using surface-enhanced Raman scattering (SERS) [2].

Silver (Ag) is one of the typical plasmon metals which is suitable for SERS. Silver SERS substrates offer a powerful technique for trace chemical and biological detection. Moreover, the morphology and size of silver nanostructures (AgNS) on SERS substrates play an essential role in amplifying the electromagnetic field and the enhancement factor (EF) of SERS substrates. The recent fabrication of the SERS substrates develops strongly with various methods and materials. The development of SERS substrates has four stages: colloid substrates, rigid substrates, flexible substrates, and universal "all-task" substrates. Unlike the intrinsic rigid, a flexible SERS substrate can be attached to rough, irregular surfaces and directly collect samples, offering a noninvasive or minimally invasive method of sample analysis. As the most natural material for flexible SERS substrates, cellulose has the advantages of easy access, low cost, eco-friendly and biodegradable [2, 3, 4].

Various physical and chemical synthetic methods have been reported to prepare AgNS both in colloid form and immobilized in other materials. One of the many preparations of Ag structures is by chemical reduction using RAs like ascorbic acid, sodium borohydride, hydrazine, sodium citrate, glucose, etc. and stabilizing agent. The capping and RAs are responsible for crystal growth that will determine the properties of the AgNS [5, 6]. Some studies about AgNS fabrication on other materials such as cellulose paper by chemical reduction also show the effect of the type of reducing agents (RAs) on the morphology and properties of AgNS [7, 8]. To fabricate AgNS on paper by chemical reduction, the paper was immersed in metal ions solution, then was reduced by RAs like $NaBH_4$ [3] and glucose [9]. However, the silver structures formed by this direct reduction method have isotropic spheres. The applications of these AgNS on paper strongly depend on the morphologies and the inter-particle distance [2]. In this paper, the morphology of AgNS on paper is controlled easily by changing the RAs. The isotropic and anisotropic morphologies of the AgNS on filter papers are produced with chitosan and RAs. They include (1) sodium borohydride ($NaBH_4$), (2) ascorbic acid (L-AA), (3) glucose, and (4) formaldehyde (HCHO). Chitosan physisorbed on the seed nanoparticle surface and after that also has shape stabilizing roles of Ag structure on paper. The synthesized paper-based SERS substrates were characterized by scanning electron microscopy (SEM) and ultraviolet-visible spectrophotometry (UV-Vis). Especially, the influence of type reducing agent on the EF and signal uniformity of SERS substrates also was determined through the Raman spectra of melamine.

2. MATERIALS AND METHODS

2.1. Materials

Silver nitrate ($AgNO_3$), sodium borohydride ($NaBH_4$), ascorbic acid (L-AA), glucose ($C_6H_{12}O_6$), formaldehyde (HCHO), sodium hydroxide (NaOH), chitosan ($C_{56}H_{103}N_9O_{39}$), citric acid ($C_6H_8O_7$) and melamine were purchased from Sigma Aldrich. The standard laboratory No.3 Whatman filter paper (porous size of 6 μm, thicknesses of 390 nm) was obtained from GE

Healthcare companies, made in the UK. The DI water was used as a working solutions (resistance > 1 MΩ).

2.2. Preparation of silver structures on paper

The schematic diagram in Figure 1 shows the fabrication process used to synthesize SERS substrates. Firstly, the filter papers were cut into 1.2 cm × 1.2 cm strips and immersed in a 3 ml aqueous solution of chitosan (10 wt.%), citric acid (10 wt.%), and 200 μl of $AgNO_3$ 0.8875 M at room temperature. After 24 hours, the complexes $[Ag(Chitosan)]^+$ on paper were reduced by $NaBH_4$, L-AA, glucose, and HCHO, dissolved in 3 ml H_2O at reaction conditions of: ratios between glucose and $AgNO_3$ of 4:1, 2000 rounds/min stirring speed and 1 min reaction time condition. The filter papers have changed from white to yellow, eventually turning dark green. The sample substrates were washed several times with DI water and then dried at 30 ^oC for 2 h in air.
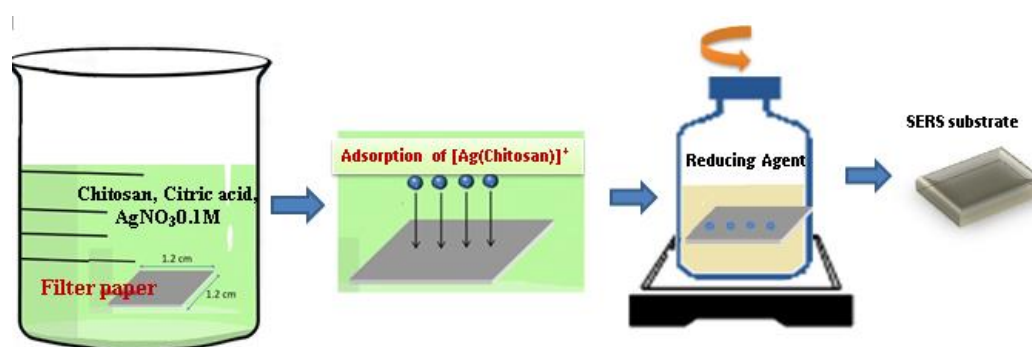
Figure 1. Schematic diagram showing the fabrication process used to synthesize Ag paper-based SERS substrates.

A series of melamine solutions with different concentrations were prepared by dissolving the melamine powders in water. A paper-based SERS substrate (3 mm × 3 mm) was dropped with 10 μl melamine solution and dried in air at room temperature before SERS analysis.

2.3. Characterization

All SEM imaging was carried out using a SEM (Hitachi S-480) equipment. The diffuse reflectance spectra of the SERS substrates were recorded using a UV-Vis spectroscope (JASCO-V570-UV-Vis-NIR). The SERS effectiveness of sample substrates were tested by using Raman spectrophotometer with He-Ne laser, wavelength of 633 nm, laser power of 10 mW, integration time of 3 s, and laser spot size of 14 μm.

3. RESULTS AND DISCUSSION

3.1. Effect of the reducing agents on the morphology of Ag structures on paper

Figure 2 shows the SEM images of AgNS on paper produced in the chitosan with different reducing agents. The morphology of AgNS obtained by using the reducing agent $NaBH_4$ give small spherical nanoparticles. With the solid reducing agent $NaBH_4$, the fabrication speed of small silver nanoparticles is very fast, about a few hundred seconds. The average size of small nanoparticles is 40 - 50 nm, and they join together to form discrete corals on filter paper fibers.

According to the publications about using $NaBH_4$ reducing agent to make silver nanoparticles in solution, the amount of sodium borohydride must be enough to stabilize the particles. Additional borohydride anions remain in the solution to stabilize the nanoparticles formed and prevent coagulation [10]. The amount of $NaBH_4$ may not be sufficient, leading to the attachment of small Ag nanoparticles, creating coral-like AgNS on the paper fiber. However, these corals do not wrap the entire surface but clump together and form scattered distribution on the filter paper fibers. When HCHO is used as a reducing agent, the AgNS on paper are also spherical. The Ag nanoparticles' average diameter is around 100 nm, which is larger than that of Ag nanoparticles obtained by using $NaBH_4$. These Ag nanoparticles are not joined together when using the $NaBH_4$ reducing agent but are distributed unevenly and scattered on the surface of cellulose fiber.

Anisotropic AgNS on the paper fibers are produced using a weak reducing agent of glucose and L-AA. At the initial stage of reducing complexes $[Ag(Chitosan)]^+$ to AgNS, the spherical shape is formed without shaking, similar to when using potent RAs such as $NaBH_4$ and HCHO. After that, small nanoparticles have grown into the anisotropic AgNS on the paper by reaction kinetics. The AgNS created on paper using glucose have a bar shape. Because, in the formation process, the crystal face (111) of small Ag nanoparticles will be given priority for development. As a result, bar-shaped AgNS on SERS substrates were obtained. In the case of using the reducing agent L-AA, the AgNS have a thin wing shape thanks to the preferential growth along the (100) crystalline plane of small silver nanoparticles.
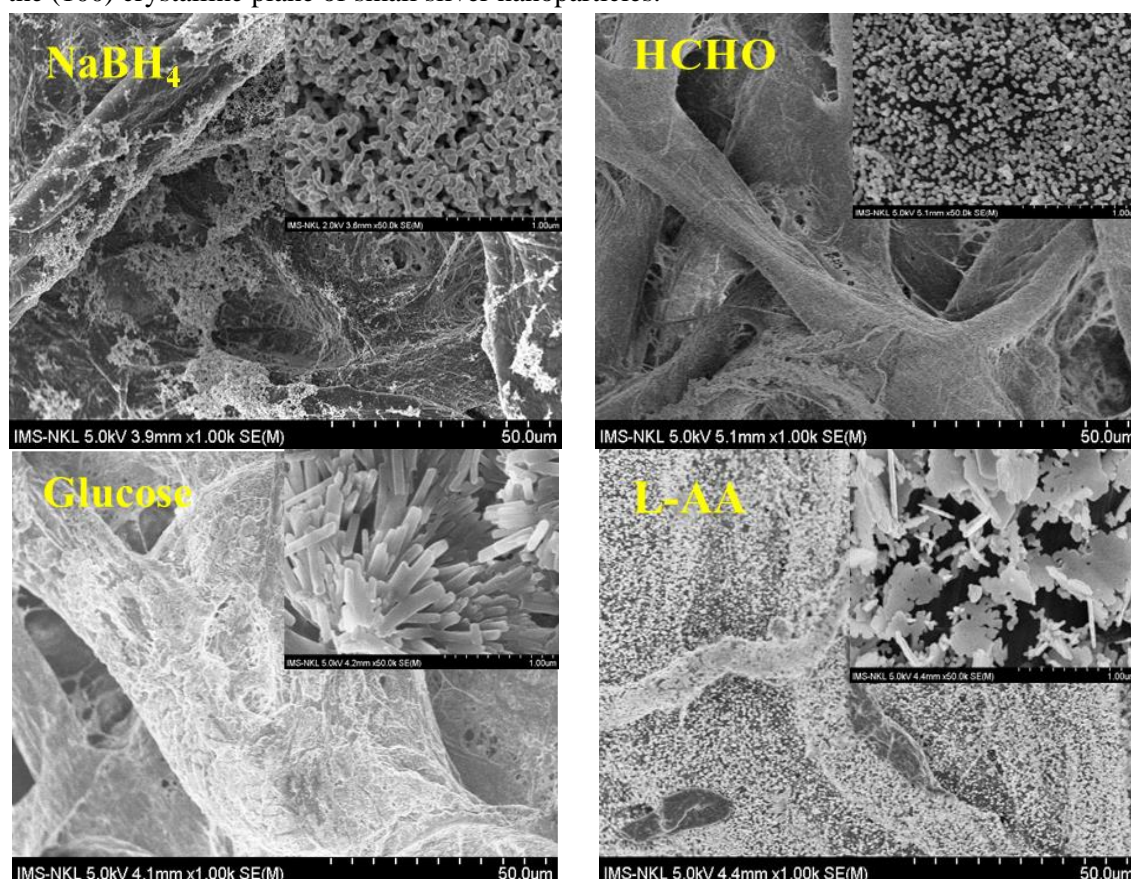
Figure 2. SEM images of AgNS on the cellulose fiber using RAs.

The difference in morphology of the AgNS on the paper fibers according to the types of RAs is due to the reaction speed of each reducing agent. Stronger RAs will usually develop AgNS to an isotropic form. In contrast, weaker RAs will give AgNS with an anisotropic appearance depending on the crystal surface development priority. By using chitosan in addition to the reduction process, the shape of AgNS on paper is more stable.

Table 1. Ag paper-based SERRS substrates compositions (wt.%) characterized by optical emission spectroscopy.

Reducing agents	Chemical elements (wt.%)		
	Ag	O	C
NaBH$_4$	19.92	45.4	34.62
HCHO	2.8	51.57	45.62
Glucose	11.38	48.49	40.13
L-AA	21.37	43.28	35.35

The formation of Ag nanostructures on paper substrates was also evaluated by EDX analysis (Table 1). The elements in the Ag paper-based SERRS substrates using reducing agents were silver, oxygen and carbon. The oxygen and carbon were from the celluloses fiber of paper substrates. However, the elemental percentage is different for each reducing agent, especially with Ag. The reducing agents, such as NaBH$_4$ and L-AA have elemental percentages of 19.92 % and 21.37 %, respectively, which are higher than the other two reducing agents. Significantly, the substrate using HCHO reducing agent has a much lower elemental percentage, i.e. of only 2.8 %. The differences in the Ag elemental percentages of specimens are similar to those obtained from SEM images.

3.2. Effect of the reducing agents on optical characterization of Ag structures on paper

The diffuse reflectance spectra of AgNS on paper produced using some of the RAs, including NaBH$_4$, HCHO, glucose, and L-AA are shown in Figure 3.
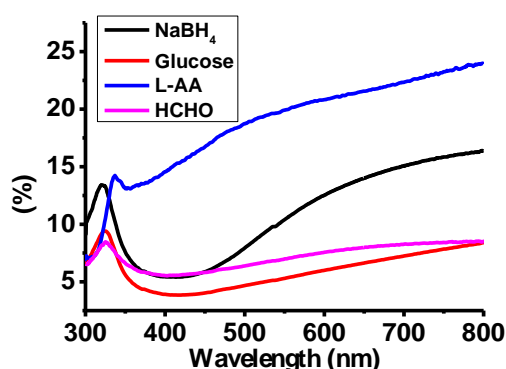
Figure 3. The diffuse reflectance spectra of the SERS substrates using different reducing agents.

The weaker reflections region in the diffuse reflectance spectra of substrates is at the wavelength region from 350 nm to 420 nm because of the substantial absorption of the AgNS on the cellulose fibers. This strong absorption region results from the dipole oscillations of the AgNS on paper. These dipole oscillations match the size of the Ag spheres on the substrate for NaBH$_4$ and HCHO RAs. These wavelength ranges correlate to the thickness of the thin wing

with L-AA RAs and the diameter of the Ag bars with glucose RAs in the case of the anisotropic AgNS. However, because the distribution of these fins is mainly horizontal rather than vertical, this dipole oscillation range did not prevail for substrates that used the L-AA reducing agent.

The reflectance at a long wavelength corresponding to high-order multipole plasmon resonance modes was observed that depended on the morphology and distribution of these AgNS on the paper. The diffuse reflectance spectra of substrates also differ in spectral half-width and intensity ratios on the long-wavelength side compared to about 400 nm. This difference is due to the effect of RAs on the morphology and distribution of the AgNS on the paper.

3.3. Effect of the reducing agents on SERS signal of AgNS on paper

Due to the structural changes of Ag on paper caused by reducing agents, the enhancement ability and reproducibility of SERS substrates are different. The analyte used is melamine which was fraudulently added to food products to increase the apparent protein content. This may lead to reproductive damage, kidney stones, or bladder cancer [11, 12]. The Raman scattering spectra of powder melamine on paper and with a concentration of 10^{-5} M on SERS substrates are shown in Figure 4. The Raman spectra of power melamine are dominated by the ring breathing vibration, observed as an intense band at 670 cm^{-1} (Figure 4b). This total symmetric stretching vibration of the ring is shifted to higher wavenumbers, about 693 cm^{-1} in the SERS spectra (Figure 4a), due to the interaction of melamine with the silver surface [12]. To compare the SERS signal of substrates using different RAs, we collected the SERS spectra of melamine at a concentration of 10^{-5} M on substrates (Fig. 4a).
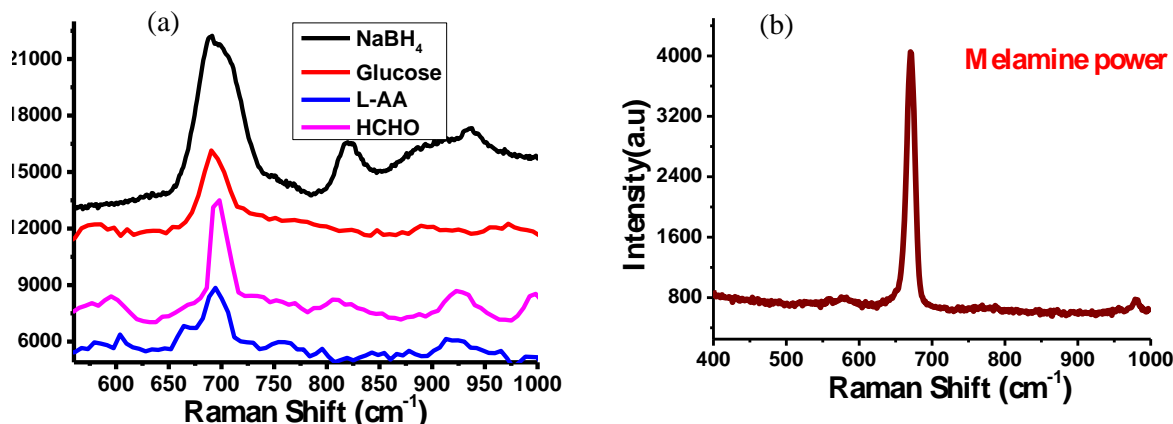
Figure 4. Measured Raman spectra for melamine (10^{-5} M) with different reducing agents (a), and Raman spectra of the melamine power measured on paper (b).

The peak intensities at 693cm^{-1} of melamine on isotropic Ag substrates used NaBH$_4$, and HCHO is higher than the anisotropic AgNS used L-AA and Glucose. This is entirely due to the number of "hot pots" on substrates, which have strong LSPR. And they are often highly localized in spatially narrow regions such as nanotips, interparticle nanogaps, or particle–substrate nanogaps [13, 14]. The tip positions of the silver nanorods produced by the use of a glucose reducing agent or the vertical silver fins produced with the L-AA reducing agent have strong LSPR. But because the tips of the Ag rods are quite large in size, about 50 nm, or in the

case of using L-AA, the large Ag thin wings of AgNS tend to lie on the surface of the cellulose fiber rather than standing up, so the number of locations with strong LSPR generated by sharp tips or edges is not much but is mainly generated by interparticle nanogaps.

The silver structures formed by $NaBH_4$ are small Ag nanoparticles connected to create a coral structure with many deep holes and narrow slits with strongly LSPR [13, 14]. Similarly, the substrate reduced by HCHO also has many hot spots generated at the nm-size distance of Ag nanoparticles on paper. In the same laser spot volume, the hotspots concentrated both in the narrow slits between the silver nanosheets and the silver nanorod tips when using glucose and were not as many as for the $NaBH_4$-reduced structures in the same projection volume. The same is true for the reducing agent L-AA . The hotpots are generated when the nanoparticles are close together for very short distances (1 - 10 nm) [13]. The holes between wing AgNS on the substrate fabricated with L-AA are pretty large, about 100 nm for the L-AA. This affects enhancing the surface Raman scattering signal of the empire fabricated by L-AA.

The SERS substrate formed by $NaBH_4$ was used to detect melamine in solution at a low concentration to find the detection limit. Raman spectra were measured for melamine solution at different concentrations from 10^{-4} M to 10^{-8} M. As shown in Figure 5, the peak at 693 cm^{-1} of melamine can be observed with a concentration of 10^{-8} M. It can be seen from Figure 5 that this technique can detect melamine at concentrations of 10^{-8} M.
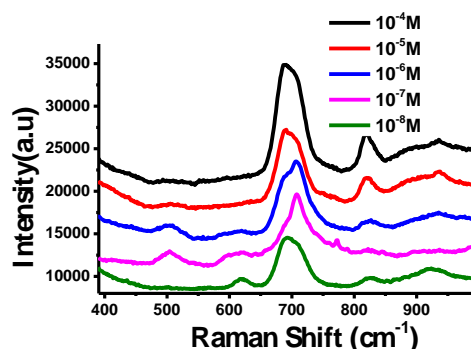
Figure 5. The limit of detection for melamine on Ag paper-based SERS substrates used $NaBH_4$ reducing agent.

The average SERS enhancement factor EF was calculated from the equation:

$$EF = \left(\frac{I_{SERS}}{I_{Raman}} \right) \left(\frac{N_{Raman}}{N_{SERS}} \right)$$

where I_{SERS} is the SERS intensity of a particular Raman line of melamine and I_{Raman} is the Raman intensity of the melamine powder on paper. N_{SERS} corresponds to the estimated number of molecules contributing to the SERS signal, while N_{Raman} is the number of molecules contributing to the Raman signal from the non-SERS surface. They are determined by the relation:

$$N_{SERS} = \eta N_A V C_{SERS} \frac{V_{laser}}{V_{SERS}} \; ; \; N_{Raman} = N_A \frac{d_{Melamine}}{M} V_{laser}$$

$$\frac{N_{Raman}}{N_{SERS}} = \frac{d_{Melamine} V_{SERS}}{\eta M V C_{SERS}}$$

where N_A is the Avogadro number, V is the total volume of solution spread on the substrate (10 µL), V_{laser} is the volume of the laser, V_{SERS} (3.51×10^{-9} m^2) is the total volume of the SERS substrate covered by the drop of melamine solution (3 mm $\times$ 3mm $\times$ 0.39 mm). $d_{Melamine}$ (1574 kg/m^3) is density of melamine. M (126.12 g/mol) is molar mass of melamine.

It can be observed from the SEM images that the total active volume with SERS only accounts for 20 % of the total volume of the laser spot ($\eta = 0.2$). Melamine powder was put on the non-SERS substrate and considered a uniform covering in the total volume of the laser spot. By applying equations, the enhancement factor of 2.3×10^9 was found.

4. CONCLUSIONS

In summary, the influence of reducing agents on the morphology and properties of silver structures on paper was investigated. The isotropic morphology of Ag structures on paper was formed by using the reducing agent such as NaBH$_4$, HCHO, and anisotropic morphology with L-AA, glucose. The morphological results of the Ag structures on the paper affect the optical properties and the Raman scattering signal. Among the four types of reducing agents, the substrates used NaBH$_4$ have the highest SERS signal with a detection limit of 10^{-8} M and EF = 2.3×10^9 for melamine.

CRediT authorship contribution statement. Nguyen Thi Bich Ngoc and Nguyen Thi Thuy: Writing, Methodology; Formal analysis; Nguyen Trong Nghia, Nguyen Duc Toan and Dao Duc Manh: Measurement; Nghiem Thi Ha Lien: Formal analysis and Review; Chu Viet Ha: Analysis and Editing.

Declaration of competing interest. The authors declare that they have no known competing financial interests or personal relationships that could have appeared to influence the work reported in this paper.

REFERENCES

1. Gui B. H., Yi H. L., Kai J. C., Hsiu Y. C., Kai C. C., and Chih M. M. - Facile Synthesis of Silver Nanoparticles and Preparation of Conductive Ink, Nanomaterials **12** (2022) 171. doi:10.3390/nano12010171

2. Liu X., Guo J., Li Y., Wang B., Yang S., Chen W., Ma X. - SERS substrate fabrication for biochemical sensing: towards point-of-care diagnostics, Journal of Materials Chemistry B, Advance Article (2021). Doi:10.1039/d1tb01299a

3. Vo T. N. L., Jungil M., Chae W. M., Vasanthan D., Jin W. O., Sung G. P., Dong H. K., Jaebum C., Yong I. L., Ho S. J. - A facile low cost paper-based SERS substrate for label free molecular detection, Sensors & Actuators: B. Chemical **291** (2019) 369-377.

4. Ruyi S., Xiangjiang L., Yibin Y. - Facing Challenges in Real-Life Application of Surface-Enhanced Raman Scattering: Design and Nanofabrication of Surface-Enhanced Raman Scattering Substrates for Rapid Field Test of Food Contaminants, Journal of Agricultural and Food Chemistry **66** (26) (2018) 6525-6543. doi: 10.1021/acs.jafc.7b03075.

5. Roto R., Hani P. R., Adhitasari S., and Nurul H. A. - Effect of Reducing Agents on Physical and Chemical Properties of Silver Nanoparticles, Indones J. Chem. **18** (4) (2018) 614-620. doi:10.22146/ijc.26907.

6. Demchenko V., Riabov S., Kobylinskyi S., Goncharenko L., Rybalchenko N., Kruk A., Moskalenko O., Shut M. - Effect of the type of reducing agents of silver ions in interpolyelectrolyte metal complexes on the structure, morphology and properties of silver containing nanocomposites, Scientific RepoRtS **10** (2020) 7126. doi: 10.1038/s41598-020-64079-0.

7. Young J. X., Lei G. Z., Xin Q., Jia Y. W. - Preparation and Charaterization of Cellulose-Silver Nanocomposites by in situ Reduction with Alkalis as Activation Reagent, Bioresources **11** (2016) 2797-2808. doi: 10.15376/biores.11.1.2797-2808.

8. Roto R., Hani P. R., Adhitasari S., Nurul H. A. - Effect of Reducing Agents on Physical and Chemical Properties of Silver Nanoparticles, Indones J. Chem. **18** (4) (2018) 614-620. doi:10.22146/ijc.26907.

9. Min L. C., Bo C. T., Jyisy Y. - Silver nanoparticle-treated filter paper as a highly sensitive surface-enhanced Raman scattering (SERS) substrate for detection of tyrosine in aqueous solution, Analytica Chimica Acta **708** (2011) 89-96. ᴅoi:10.1016/j.aca.2011.10.013.

10. Liliana M., Denisa F., Ovidiu O., Alexandru M., Anton F., Ecaterina A., Alina M. H. - Optimized Synthesis Approaches of Metal Nanoparticles with Antimicrobial Applications, Journal of Nanomaterials, **6651207 (**2020**)**, 14 pages. doi:10.1155/2020/6651207.

11. Panneerselvam R., Wei L. Tang., Jyisy Y. - Rapid detection of Melamine in milk liquid and powder by surface-enhanced Raman scattering substrate array, Food Control **56** (2015) 155-160. doi:10.1016/j.foodcont.2015.03.028.

12. Nicoleta E. M., Mircea O., Vasile C., Nicolae L. - FTIR, FT-Raman, SERS and DFT study on melamine, Vibrational Spectroscopy **62** (2012) 165-171. doi:10.1016/j.vibspec.2012.04.008.

13. Yong, Z., Lei. D.Y., Lam, C.H. - Ultrahigh refractive index sensing performance of plasmonic quadrupole resonances in gold nanoparticles, Nanoscale **9**, 187, (2014), 6 pages, doi: 10.1186/1556-276X-9-187.

14. Song Y. D., En M. Y., Zhong Q. T., Martin M., - Electromagnetic theories of surface-enhanced Raman spectroscopy, Chem. Soc. Rev. **46** (2017) 4042. doi:10.1039/7cs00238f.